Plasmon-free polymeric nanowrinkled substrates for surface-enhanced Raman spectroscopy of two-dimensional materials

Marziye Mirbagheri, Ph.D.**,†,‡,¶,§ Jasneet Kaur, Ph.D.**,† Hoang Vu Pham,†,‡,¶ Vahid Adibnia, Ph.D.,§ Hadis Zarrin, Ph.D.,† Xavier Banquy, Ph.D.,§ and Dae Kun Hwang, Ph.D.*,†,‡,¶

†*Department of Chemical Engineering, Faculty of Engineering & Architectural Science, Ryerson University, Toronto, Ontario M5B 2K3, Canada*

‡*Keenan Research Center, Li Ki Shing Knowledge Institute, St. Michael's Hospital, Toronto, Ontario M5B 1W8, Canada*

¶*Institute for Biomedical Engineering, Science and Technology (iBEST), St. Michael's Hospital, Toronto, Ontario M5B 1W8, Canada*

§*Faculty of Pharmacy, Université de Montréal, C.P. 6128, succursale Centre Ville, Montreal, Quebec H3C 3J7, Canada*

E-mail: dkhwang@ryerson.ca

* Corresponding author

** These authors equally contributed to this work.

Abstract

We report plasmon-free polymeric nanowrinkled substrates for surface-enhanced Raman spectroscopy (SERS). Our simple, rapid and cost-effective fabrication method involves depositing a poly(ethylene glycol) diacrylate (PEGDA) prepolymer solution droplet on a fully polymerized, flat PEGDA substrate, followed by drying the droplet at room conditions and plasma treatment, which polymerizes the deposited layer. The thin polymer layer buckles under axial stress during plasma treatment due to its different mechanical properties from the underlying soft substrate, creating hierarchical wrinkled patterns. We demonstrate the variation of the wrinkling wavelength with the drying polymer molecular weight and concentration (direct relations are observed). A transition between micron to nanosized wrinkles is observed at 5 v% concentration of the lower molecular weight polymer solution (PEGDA Mn 250). The wrinkled substrates are observed to be reproducible, stable (at room conditions) and, specially, homogeneous at and below the transition regime, where nanowrinkles dominate, making them suitable candidates for SERS. As a proof-of-concept, the enhanced SERS performance of micro/nano-wrinkled surfaces in detecting graphene and hexagonal boron nitride (h-BN) is illustrated. Compared to the SiO_2/Si surfaces, the wrinkled PEGDA substrates significantly enhanced the signature Raman bands intensities of graphene and h-BN by a factor of 8 and 50, respectively.

1 Introduction

The surface-enhanced Raman spectroscopy (SERS) is an attractive tool for sensing molecules in trace amounts in the chemical[1] and biochemical[2] analytics. The surface-enhanced Raman spectra was initially observed in 1974, when Fleischmann et al.[3] reported the first high-quality Raman spectra of monolayer-adsorbed pyridine on an electrochemically roughened silver electrode surface. While there is still no consensus on the exact Raman signal enhancement mechanism in SERS using metallic platforms, two primary theories are largely accepted: the electromagnetic and chemical enhancement[4,5]. The strong electromagnetic field enhancement at the surface of

nanostructured metallic particles is related to the plasmonic effects, which are produced by the interactions between the electromagnetic waves (i.e., laser light) and metallic nanostructures[6].

Metallic nanoparticles have been widely investigated in SERS mainly due to their simple and cost-effective production. The most commonly used fabrication approach for metallic nanoparticles is the reduction of metal cations from their salts. For example, the reduction of silver disulfite using various reducing agents, such as hydroquinone, produces silver colloids[7], whereas gold colloids can be obtained through the reduction of chloroauric acid by citrate, known as the Turkevich method[8]. The nanoparticle size, shape, aggregation properties, and surface charge properties, with determining roles in the SERS efficiency, can be manipulated by varying the temperature, reactant concentrations, and ionic strength[7,9,10]. Nevertheless, despite the recent progress in the field of nanoparticle-based SERS, the structural controllability and hot-spot formation in the detection zone of metallic nanoparticles remain challenging, resulting in conflicting SERS signals[5,11].

Recently, researchers have been exploring three-dimensional platforms with increased adsorption of analyte molecules and hot-spot formation. In contrast to low-dimensional geometries, the laser confocal volume in a three-dimensional space can create a stronger SERS response by increasing the average field enhancement and the generation/collection of SERS signals. (In a three-dimensional space, the hot-spot area is larger compared to one- and two-dimensional platforms.) The three-dimensional SERS platform fabrication involves two common methods. In the first approach, the three-dimensional structures are constructed using plasmon-free organic or inorganic materials via template-wetting[12], electrospinning[13], lithography[14] and so forth. Next, the three-dimensional supports are functionalized using plasmonic nanoparticles or thin films[15–17]. Alternatively, the three-dimensional SERS platforms could be manufactured directly using plasmonic materials. For example, self-assembly of colloidal plasmonic particles into well-organized three-dimensional structures is one of the simplest and most effective approaches for creating higher-dimensional SERS substrates[18].

In the past few years, inorganic and organic semiconductors and carbon-based π-conjugated SERS structures have been introduced as potential non-metallic SERS platforms[19–21]. For example, Alessandri[22] reported enhanced Raman scattering using TiO_2 shell-based spherical resonators in the absence of plasmonic enhancers. The improved Raman SERS performance in the core-shell microspheres was attributed to the effective internal reflection through the spheres, yielding evanescent electromagnetic fields that generate local surface hot spots. Compared to metallic and inorganic substrates, limited studies have reported graphene-enhanced Raman scattering[23,24]. In a very recent work, a quasi-equilibrium plasma-enhanced chemical vapor deposition method was used to produce highly crystalline, atomically clean graphene quantum dots directly on Si–SiO_2 with sizes down to 2 nm[25]. The graphene quantum dots-based substrates were directly used as a SERS platform showing enhancement factors up to 2.37×10^3 with rhodamine 6G, which is much higher than those on conventional graphene sheets. However, the fabrication of these non-metallic platforms as well as the three-dimensional metallic structures is expensive and technologically demanding. Therefore, the development of alternative approaches is of great interest not only to widen the SERS applications but also to further elucidate fundamental questions.

In this paper, we report a very simple and rapid approach for creating plasmon-free, polymeric SERS substrates comprising nano- and micro-scale wrinkling patterns. The nanosized wrinkles in the range of 100–1000 nm may also be referred to as sub-micron. However, in this paper, for the ease of discussion, below 1 μm is referred to as nanosized. The fabrication method includes drying a PEGDA prepolymer solution on a fully polymerized, flat PEGDA surface, followed by plasma treatment, leading to formation of the wrinkling patterns. Various factors such as polymer molecular weight and concentration are introduced as controlling parameters for wrinkling size. As a proof-of-concept, the wrinkled polymeric platforms are used to assess the Raman signals of graphene and hexagonal boron nitride (h-BN). Graphene is a semi-metallic transparent two-dimensional network of sp^2 carbon atoms in a hexagonal honeycomb lattice with strong co-

valent bonds. Few-layered or monolayered graphene exhibits intriguing properties, such as large electrical and thermal conductivity, high mechanical strength and high optical transparency[26]. h-BN, also known as white graphene, is a two-dimensional insulator with a wide bandgap (> 6eV) and an atomic structure similar to that of graphene where boron and nitrogen atoms alternate at the vertices of a planar hexagonal sp^2 network[27]. h-BN is uniquely featured by its exotic opto-electrical properties together with mechanical robustness, thermal stability, and chemical inertness[28]. Raman spectroscopy is often used to determine the thickness and crystallinity of two-dimensional materials, such as graphene (with the characteristic D, G, and 2D bands) and h-BN, which exhibits only one Raman band corresponding to the E_{2g} vibration mode[29–31]. In addition, the Raman signals from BN are much weaker than those from carbon materials[31]. The considerable Raman signal enhancements on the wrinkled organic substrates are compared with those on standard SERS substrates , *i.e.*, SiO_2/Si wafer (Si with 300 nm of SiO_2), and smooth PEGDA substrates.

2 Results and discussion

2.1 SERS substrate fabrication

We firstly demonstrate the fabrication of micro/nano-wrinkled surfaces via plasma treating a thin, dried layer of a prepolymer solution on a fully polymerized substrate, as illustrated in Figure 1. Here, poly(ethylene glycol) diacrylate Mn 700 (PEGDA700) was used to fabricate the supporting substrate. Therefore, 0.4 μl of PEGDA700 in pure ethanol solution was sandwiched between a clean coverglass and a microfluidic channel (height = 100 μm), photopolymerized, washed and dried sequentially. The resulting surface, with a roughly circular cross-section, had a diameter of ~ 2 mm and a height of 100 μm, which can be varied based on the prepolymer solution volume and microfluidic channel height.

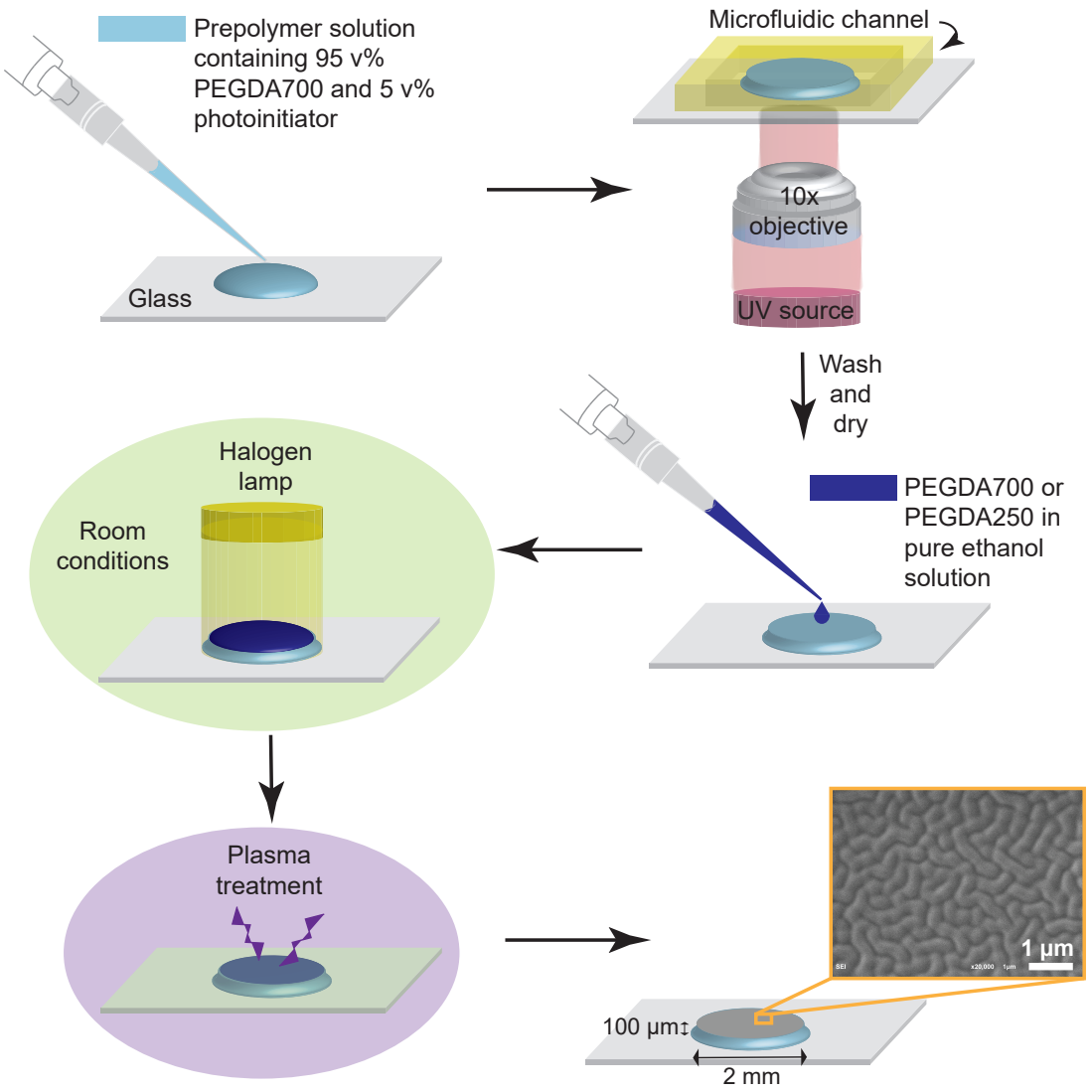

Figure 1: Formation sequence of wrinkled surfaces. Starting from top, left panel, the flat and circular support is fabricated by sandwiching 0.4 μl of the PEGDA700 prepolymer solution between a clean coverglass and a microfluidic channel with a height of 100 μm, followed by photopolymerization. The flat support is then extensively washed and dried, onto which 0.5 μl of the PEGDA700 or PEGDA250 in pure ethanol solution is dispensed. The deposited prepolymer layer is then immediately dried under a specific condition for 2 minutes. The deposited polymer is then polymerized by plasma treatment, leading to the formation of nano/micro-wrinkles with various wavelengths that depend on the polymer concentration and molecular weight.

To create the wrinkling patterns, 0.5 μl of PEGDA700 or poly(ethylene glycol) diacrylate Mn 250 (PEGDA250) in pure ethanol solution was dried onto the flat supports under specific

conditions (details in the Experimental section). The drying process was governed by the coffee-ring effect during the evaporation of the polymer particles suspension on a polymer surface with favourable particle-surface interactions. Generally, the coffee-ring effect depends on various parameters, such as particle size and shape, the particle-surface interaction, the evaporation rate, the droplet volume, *etc.*

The coffee-ring effect during the drying of a PEGDA solution on a fully polymerized PEGDA surface was extensively studied and explained in a previous paper by our group[32]. Briefly, the evaporation starting from the droplet periphery is firstly governed by the capillary flow, leading to the accumulation of the polymer solution at the edges of the substrate. At this stage, the air–liquid interface shape deviates from hemisphere to a cutaway ring torus. A higher polymer concentration at the peripheries results in a local surface-tension gradient (increasing toward the center), which encourages the Marangoni flow that carries the polymers backward to the center. Moreover, the Marangoni flow induces a contact line recession toward the center. Therefore, the final polymer deposition covers the entire surface with a small gap at the edges.

Finally, the hierarchical wrinkling patterns are formed by polymerizing the deposited prepolymer on the surface using plasma treatment. The buckling of the thin crosslinked polymer layer on the support, due to their different mechanical properties, creates the wrinkles[33,34]. In a recent paper, Rofouie et al.[35] explained the formation of the surface wrinkling patterns and their variation based on an interplay between bending elasticity and compressive strain.

2.2 SERS substrate characterization

To propose the wrinkled substrates as potential candidates for SERS, several properties are required. Firstly, the majority of the wrinkling patterns must be preferably nanosized to maximize

the hot-spot zone (surface contact). The wrinkling wavelength, λ, can be determined using[33]

$$\lambda \approx 2\pi h \left(\frac{E_f}{3E_s} \right)^{(1/3)} \tag{1}$$

where h is the polymer layer thickness, and E_f and E_s are the elastic moduli of the viscoelastic supporting surface and of the thin polymer layer, respectively. The wrinkle amplitude, A, is related to λ using[33]

$$A \approx \lambda \left(\frac{\sqrt{1+\nu}}{\pi} \sqrt{\mid \epsilon \mid - \epsilon_c} \right) \tag{2}$$

where ν is the Poisson ratio and ϵ is the strain with $\epsilon_c = 0.52(E_s/E_f)^{2/3}$ the critical strain above which the wrinkles start to appear. While the thin polymer layer thickness can be varied by the polymer concentration, its elastic modulus can be manipulated by varying the polymer molecular weight. Knowing that the polymer elastic modulus is inversely proportional to molecular weight[36], we were able to approach nanosized wrinkling patterns by using PEGDA250 instead of PEGDA700, as demonstrated in Figure 2. When preserving all other parameters and conditions,

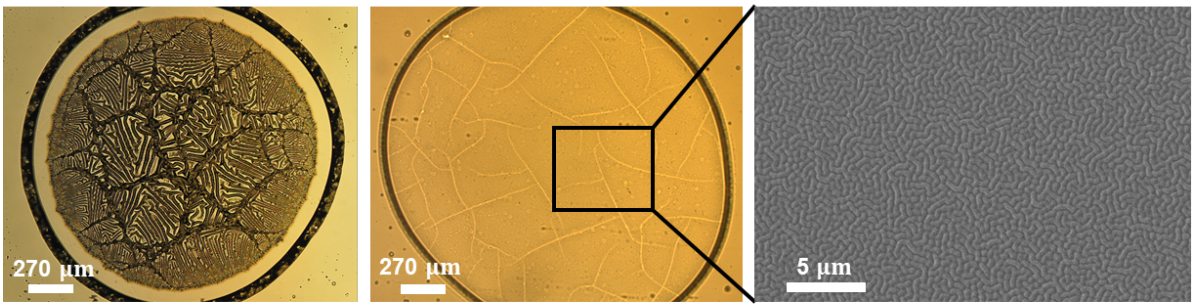

Figure 2: Effect of polymer molecular weight on wrinkling wavelength. The drying prepolymer solution is 3 v% PEGDA700 (a) or 3 v% PEGDA250 (b and c) in pure ethanol. All other conditions and parameters are the same. The microwrinkles in panel (a) were visible using brightfield imaging, whereas the nanowrinkles in panel (b) were observable using scanning electron microscopy (SEM), as shown in panel (c).

the lower polymer molecular weight resulted in smaller wavelengths, down to $\sim 370 \pm 20$ nm

for 3 v% PEGDA250 solution. Here, the reported wavelength is based on 5 measurements at different positions on Figure 2 (c) using ImageJ (an example of such analysis is found in the SI). The polygonal closed domains in Figure 2 (a and b) are formed by the topological defects of the wrinkle field, as was explained by Kim et al.[33]. As the compression of the top polymer layer continues during the plasma treatment, the wrinkling patterns start to fold simultaneously throughout the surface. The folds propagate through the surface, split when encountering the topological defects of the wrinkle field and connect to each other, producing a network of polygonal domains. Consequently, new wrinkles appear within each individual domain in accordance to the local stress distribution.

The wrinkling size also depends on the polymer concentration (the thin polymer layer thickness). Thus, examining the wrinkling formation for PEGDA250 concentrations varying from 2 to 7 v%, we observed a transition regime at which micro-sized wrinkling wavelengths started to appear. According to Figure 3, the nanowrinkles sizes increase with PEGDA250 concentration and the transition regime occurs at PEGDA250 concentration 5 v%, where a mix of nano- and micro-wrinkles are obtained. Above 5 v% concentration, the percentage of microwrinkles increases with polymer volume fraction in the solution.

In should be noted that the wrinkling formation depends on the ratio E_f/E_s. For example, on a rigid supporting surface ($10^2 < E_f/E_s \lesssim 10^3$) and at large values of strain ($\mid \epsilon \mid \gtrsim 0.2$), wrinkles are preserved during formation, producing multi-periodic patterns, such as those shown in the present paper. However, for viscoelastic layers ($E_f/E_s \gtrsim 10^4$), it has been observed that the formation of localized single folds relaxes and eliminates the neighbouring wrinkles[33]. Therefore, it is expected that there exists a threshold for the polymer molecular weight and concentration, above which stable wrinkling patterns will not be achievable.

Another imperative property for SERS surfaces in addition to periodic nanosized wrinkles is the substrate homogeneity. As shown in Figures 2 and 3 (g), respectively, the wrinkles become

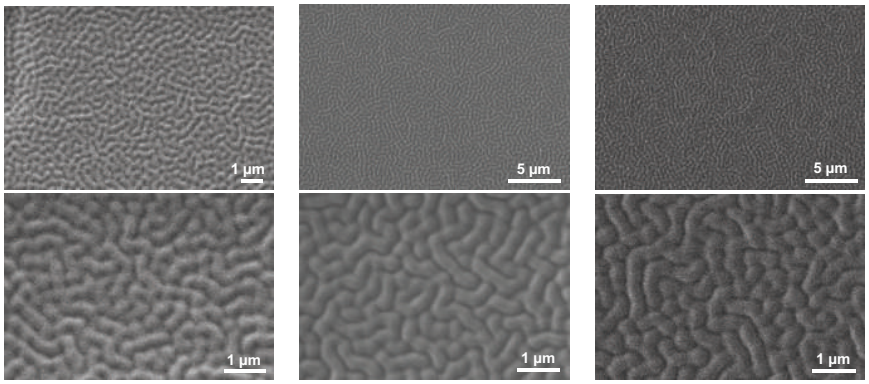

(a):PEGDA250 2 v% (b):PEGDA250 3 v% (c):PEGDA250 4 v%

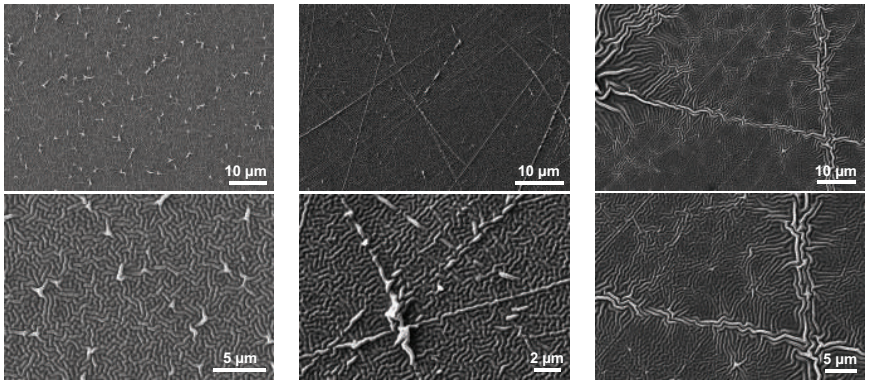

(d):PEGDA250 5 v% (e):PEGDA250 6 v% (f):PEGDA250 7 v%

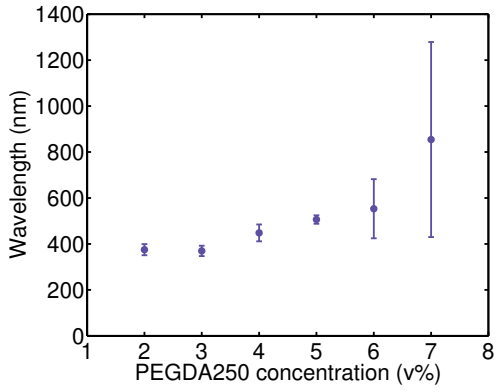

(g)

Figure 3: Effect of PEGDA250 concentration on wrinkling wavelength. The wrinkling wavelength transition regime occurs at 5 v% polymer concentration. (g) The wrinkling wavelengths are estimated based on 5 measurements at different positions on the higher magnification images in panels (a)–(f) using ImageJ (an example of such measurement is provided in the SI). The error bars display the standard deviations from the mean values.

increasingly heterogenous for higher polymer molecular weight and polymer concentrations. In other words, the surface homogeneity is only achievable with PEGDA250 concentration ≤ 5 v%, where interestingly the nanowrinkles are also dominating. To confirm this, using scanning electron microscopy (SEM), we probed the surfaces of two representative samples, namely PEGDA250 3 v% and PEGDA250 5 v%.

Figure 4 illustrates that nanowrinkles are fairly homogenous throughout the surface, with the mix of nano- and micro-wrinkles being slightly larger at the center than those at the edges of the surface. Here, for PEGDA250 3 v% and PEGDA250 5 v%, respectively, the averaged wrinkling wavelengths across the surface and based on Figure 4 are 398 ± 52 and 497 ± 104 nm. These values are reported according to estimated wavelengths at 5 different positions on the substrates. The increasing wrinkle size towards the center of the samples can be attributed to the coffee-ring effect during the drying of the polymer solution. As explained above, during the second phase of the drying, the Marangoni flow carries the polymers toward the center. The higher surface heterogeneity for higher polymer concentrations and polymer molecular weights indicates that the local polymer concentration gradient increases with these parameters, giving larger wrinkles at the center.

Other important features of a SERS substrate are stability and reproductivity. Our repeated sample preparation and characterization confirmed that the surface characteristics including wrinkling size and homogeneity are reproducible and stable for days (we observed them for 10 days). In the following section, we examine the SERS performance of the nano/micro-wrinkled surfaces in characterizing graphene and h-BN.

2.3 Raman spectroscopy of graphene and h-BN on nano/micro-wrinkled and smooth polymer substrates

In order to acquire the Raman spectroscopy of graphene and h-BN on a representative wrinkled

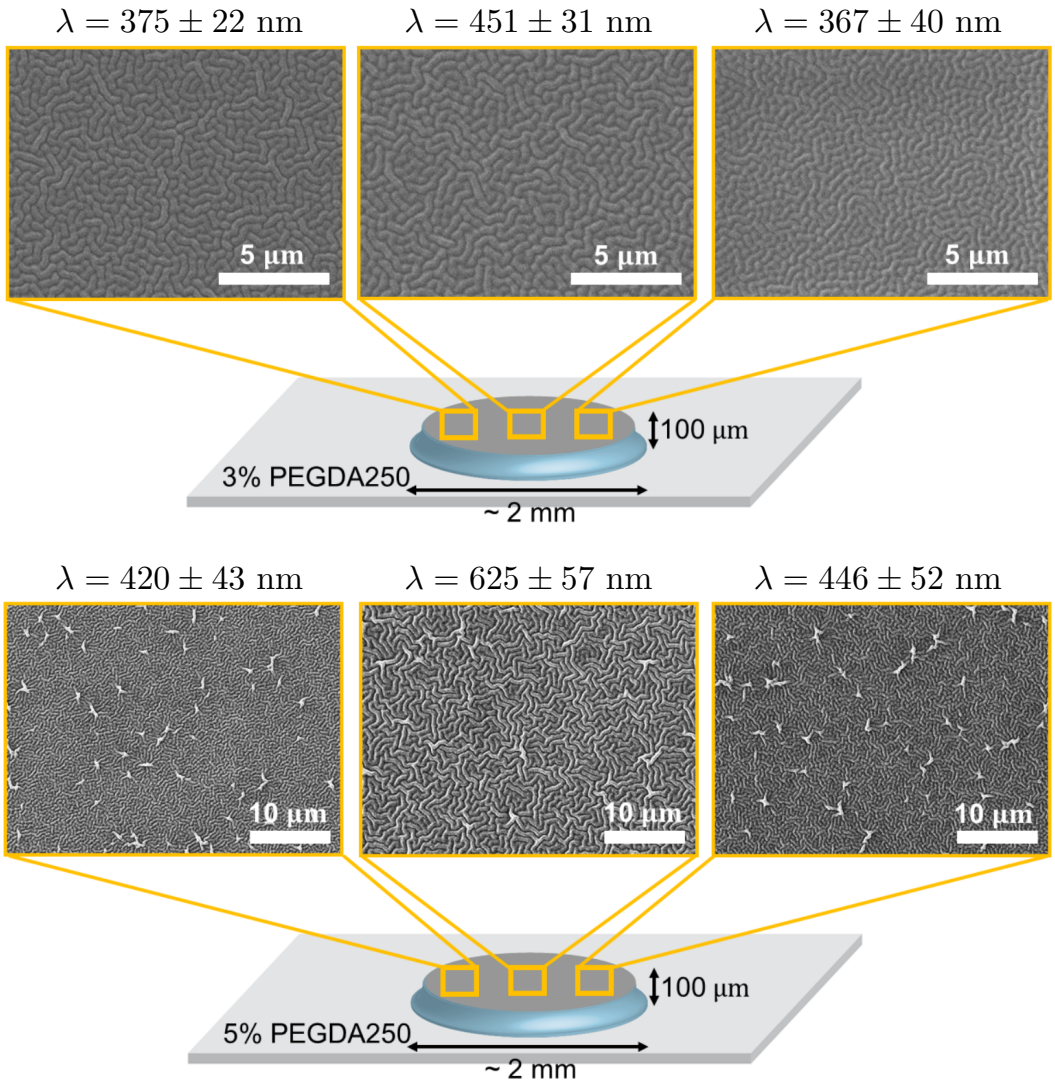

Figure 4: Wrinkling pattern homogeneity for various PEGDA250 concentrations, *i.e.*, 3 (top) and 5 v% (bottom). As the wrinkling size grows for higher concentrations, the wrinkling wavelength becomes slightly larger at the center compared to the edges. Here, the averaged wrinkling wavelengths across the surfaces of PEGDA250 3 v% and 5 v% are 398 ± 52 and 497 ± 104 nm, respectively, which are reported as means and standard deviations of the measurements.

5 v% PEGDA250 substrate, these samples were deposited on the substrate and excited with laser under a confocal microscope. Similarly, graphene and h-BN were deposited on the smooth PEGDA and SiO_2/Si substrates to compare their Raman signals intensities. Note that the chemical compositions of the smooth and wrinkled PEGDA surfaces are identical, as was confirmed in our previous

work[37]. The visibility of graphene and h-BN peaks depends greatly on the substrate interference effects, which vary based on the thickness of SiO_2 on Si and the laser excitation energy[38,39]. Here, the characteristic conditions for Raman spectroscopy of graphene and h-BN (532 nm excitation laser and Si with 300 nm of SiO_2) were used[40–42].

In graphene, the Stokes phonon energy shift, caused by laser excitation, creates three main peaks in the Raman spectrum: the G band (1580 cm^{-1}), which is a primary in-plane vibrational mode, the 2D band (2690 cm^{-1}), which is a second-order overtone of a different in-plane vibration, and the D band (1350 cm^{-1})[43]. The E_{2g} band frequency of bulk h-BN crystals is observed at 1366.8 $\pm$ 0.4 cm^{-1}, which is the characteristic spectroscopic signature represented by the E_{2g} phonon mode[41,42].

Figure 5 shows the Raman spectra of deposited graphene and h-BN on wrinkled PEGDA surface compared with those on the smooth PEGDA and SiO_2/Si substrates. The presence of the D, G and 2D bands of graphene on the wrinkled PEGDA surface are observed at 1345 cm^{-1}, 1588 cm^{-1} and 2690 cm^{-1}, respectively, which are $\sim$ 8 times higher than those on the smooth PEGDA and SiO_2/Si substrates with peak values remaining the same. The E_{2g} band of h-BN is exhibited by a sharp peak on the wrinkled PEGDA substrate, whereas it is hardly detectable on the SiO_2/Si surface. The intensity of E_{2g} band of h-BN on the SiO_2/Si surface is $\sim$ 500 counts, which is enhanced on the wrinkled PEGDA by a factor of 50. On the other hand, the intensity of h-BN Raman spectra on the wrinkled PEGDA is $\sim$ 5 times higher compared to that on the smooth PEGDA.

The SERS effect on wrinkled polymeric surfaces compared to the smooth polymer and SiO_2/Si substrate can be explained by, firstly, the wrinkled surface topography that creates signal enhancing hot spots in the narrow valleys between the wrinkles. Secondly, the wrinkling increases the surface area of the polymer and, thus, improves the sample adsorption[31]. The third possible mechanism of enhancement is the intrinsic roughness of the polymer surface[44]. However, this

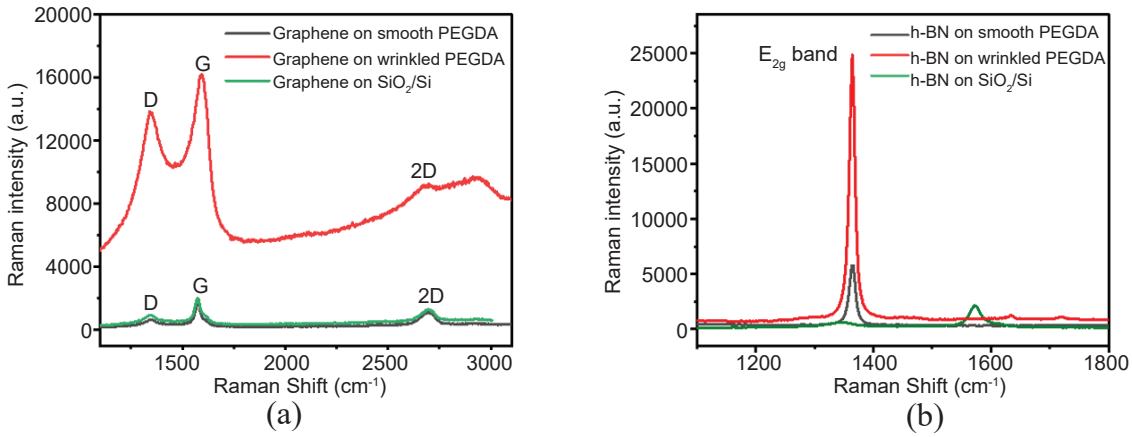

Figure 5: Raman spectra of (a) graphene and (b) h-BN on the smooth PEGDA, wrinkled PEGDA and SiO_2/Si substrates.

proof-of-concept work evaluating the SERS capabilities of wrinkled PEGDA surfaces should be complemented by future experimentations to explore the influence of various wrinkling characteristics, such as wrinkling wavelength, amplitude and surface roughness, on the Raman spectroscopy enhancement factor. It is expected that smaller wavelengths and larger amplitudes increase the enhancement factor provided that the aforementioned mechanisms are indeed responsible for the observed SERS effect. In addition, the present study was focused on the few-layered graphene and h-BN samples due to their widespread applications, however, several previous investigations have reported the impact of the layer number of two-dimensional materials on their Raman signal intensities[45,46]. Therefore, future studies should also be undertaken to explore the SERS effect of wrinkled polymeric surfaces with single-, bi-, tri- and few-layered materials, which should include not only graphene and h-BN but also others such as transition metal dichalcogenides (TMDCs).

3 Conclusion

A plasmon-free nanowrinkled substrate is created using a simple, rapid and cost-effective approach. Briefly, a prepolymer in ethanol solution is dried on a fully polymerized flat substrate, followed

by polymerizing the deposited prepolymer layer using plasma treatment, leading to the formation of wrinkling patterns via the buckling of the thin polymer layer on the soft support surface due to their different mechanical properties. The wrinkling wavelength is varied from micro- to nano-scale by manipulating the polymer molecular weight (the mechanical property of the thin polymer layer) and the polymer concentration (the thickness of the thin polymer layer). In general, lower molecular weight and concentrations lead to smaller wrinkles, where a mixture of micro and nano-wrinkles are obtained at and above the transition regime corresponding to 5 v% of the lower molecular weight polymer. The wrinkled organic substrates are observed to be reproducible, stable (at room conditions) and fairly homogeneous, with the latter only at and below the transition regime.

The homogeneous micro/nano-wrinkled polymeric substrates are then used in SERS to explore their enhanced Raman performance in detecting graphene and h-BN compared to the smooth polymer and the standard SiO_2/Si surfaces. Therefore, the micro/nano-wrinkled polymeric substrates can exhibit a great potential for SERS of various layered two-dimensional nanostructures, such as graphene and h-BN.

4 Experimental Section

Fabrication of planar surfaces for supporting the nano- and micro-wrinkled patterns: To fabricate the nano- and micro-wrinkled substrates, firstly, the planar supporting surfaces with roughly circular shapes and diameter of $\sim$ 2 mm were fabricated using photolithography. Poly(ethylene glycol) diacrylate Mn 700 (PEGDA700, Sigma Aldrich) was chosen as the building block of the supporting structures. Therefore, 0.4 μl of PEGDA700 prepolymer solution containing 5% 2-hydroxy-2-methylpropiophenon photoinitiator (Darocur 1173, Sigma Aldrich) was sandwiched between a clean coverglass and a microfluidic channel with a rectangular cross-section and a height of 100 μm. Standard soft-lithographic techniques were used to fabricate the microfluidic chan-

nels by curing a mixture of polydimethylsiloxane (PDMS, Sylgard 184, Dow Corning) precursor and the curing agent (10:1) on a patterned SU-8 photoresist (MicroChem). The planar surface was then photopolymerized using a metal arc lamp as an ultraviolet (UV) source (Lumen 200, Prior Scientific, Rockland, MA, USA). A UV shutter (Lambda SC, Sutter Instruments, Novato, CA, USA) was installed in the UV light path to control the UV exposure time, which was set to 2000 ms. The UV shutter was controlled by a LabVIEW program (National Instruments, Austin, TX, USA) through a digital controller (NI 9472, National Instruments, Austin, TX, USA). An inverted microscope Axio Observer (Carl Zeiss, Jena, Germany) was used as the photopolymerization platform. A UV filter set (11000v3, Chroma, VT, USA) was used to obtain desired UV excitation for polymerization (305-390 nm). Next, the microfluidic channel was peeled off and the planar circular support was extensively washed with ethanol 100% in a drop-by-drop fashion to remove any unpolymerized monomer, dried in room condition and used as explained in the following section.

Formation of the nano- and micro-wrinkled patterns: To synthesize the wrinkling patterns, each planar surface was placed on a microscope stand (Axio Observer, Carl Zeiss, Jena, Germany) at $\sim$ 7 cm distance from the microscope Halogen lamp (100 W and 12 V), which was perpendicularly illuminating the center of the structure at full power. This was to maintain a specific drying condition for the PEGDA700 or poly(ethylene glycol) diacrylate Mn 250 (PEGDA250, Sigma Aldrich) solution on the supports. Therefore, 0.5 μl of the prepolymer solution containing various concentrations of PEGDA700 or PEGDA250, ranging from 2 to 7 v%, in pure ethanol (no photoinitiator) was carefully pipetted onto the planar structure and dried at room condition for $\sim$ 2 minutes. Finally, after evaporation, each substrate was treated with plasma (Harrick Plasma, PDC-32G, NY) for 5 seconds, to produce the wrinkling patterns by crosslinking the dried polymers. Detailed information regarding the formation mechanism of these wrinkles are found in the literature[33,47].

Materials characterization: The brightfield microscopy was conducted using an inverted microscope Axio Observer (Carl Zeiss, Jena, Germany), and the images were analyzed using the ZEN lite software (Carl Zeiss, Jena, Germany). Moreover, scanning electron microscopy (SEM, JEOL 6610LV Scanning Electron Microscope) was used to image the wrinkling patterns, which were coated with 20–30 nm of gold.

Surface-enhanced Raman spectroscopy: Pristine graphene flakes were purchased from Carbon masters. The graphene sample has thickness of 4–5 layers and lateral size of 1–5 μm. Bulk h-BN (hexagonal boron nitride powder $\sim$ 1 μm) and isopropanol were purchased from Sigma-Aldrich Inc. The bulk h-BN was dispersed in isopropanol and exfoliated by liquid phase exfoliation to synthesize two-dimensional h-BN nanoflakes[42]. The h-BN sample has thickness of 3–5 layers with lateral size of 80–130 nm. Bare SiO_2/Si stands for the blank SiO_2/Si wafer (Si with 300 nm of SiO_2) without any deposited sample on it.

The confocal Raman microscope with specification of Renishaw via Confocal Raman Spectrometer was built around a Leica DMI6000 automated epifluorescence microscope. The Renishaw confocal Raman microscope with solid state excitation source of 532 nm, allows for spatially resolved spectroscopy to be carried out in a confocal manner at high speed. Oxidized silicon crystal (Si/SiO_2, Si with 300 nm of SiO_2) was used for calibration. The wrinkled polymeric substrate was observed to be a flat stub under the optical microscope. Raman peak of Si/Sio_2 crystal was calibrated at 520 ± 0.5 cm^{-1}. The laser power was controlled below 1 mW to avoid the decomposition of molecules and the heating effect. To ensure consistency, multiple scans of Raman spectra over different areas of graphene and h-BN samples were acquired.

Acknowledgements

Support from CRC (Canada Research Chairs program) and NSERC (Natural Sciences and Engineering Research Council of Canada) to X. B. and D. K. H., FRQNT and TransMedTech post-

doctoral research scholarship to M. M. and V. A., and Mitacs Elevate postdoctoral fellowship to J. K. is gratefully acknowledged.

Conflict of Interest

The authors declare no conflict of interest.

Keywords

surface-enhanced Raman spectroscopy, nano-microscale wrinkling, coffee-ring effect, hierarchical material, microfluidics, graphene.

References

(1) Schlücker, S. Surface-enhanced Raman spectroscopy: Concepts and chemical applications. *Angew. Chem. Int. Ed.* **2014**, *53*, 4756–4795.

(2) Cialla-May, D.; Zheng, X.-S.; Weber, K.; Popp, J. Recent progress in surface-enhanced Raman spectroscopy for biological and biomedical applications: from cells to clinics. *Chem. Soc. Rev.* **2017**, *46*, 3945–3961.

(3) Fleischmann, M.; Hendra, P. J.; McQuillan, A. J. Raman spectra of pyridine adsorbed at a silver electrode. *Chem. Phys. Lett.* **1974**, *26*, 163–166.

(4) Cialla, D.; März, A.; Böhme, R.; Theil, F.; Weber, K.; Schmitt, M.; Popp, J. Surface-enhanced Raman spectroscopy (SERS): Progress and trends. *Anal. Bioanal. Chem.* **2012**, *403*, 27–54.

(5) Demirel, G.; Usta, H.; Yilmaz, M.; Celik, M.; Alidagi, H. A.; Buyukserin, F. Surface-enhanced Raman spectroscopy (SERS): An adventure from plasmonic metals to organic semiconductors as SERS platforms. *J. Mater. Chem. C* **2018**, *6*, 5314–5335.

(6) Ru, E. L.; Etchegoin, P. *Principles of Surface-Enhanced Raman Spectroscopy: and related plasmonic effects*; Elsevier Science: Oxford, UK, 2008.

(7) Prucek, R.; Panacek, A.; Soukupova, J.; Novotny, R.; Kvitek, L. Reproducible synthesis of silver colloidal particles tailored for application in near-infrared surface-enhanced Raman spectroscopy. *J. Mater. Chem.* **2011**, *21*, 6416–6420.

(8) Kimling, J.; Maier, M.; Okenve, B.; Kotaidis, V.; Ballot, H.; Plech, A. Turkevich method for gold nanoparticle synthesis revisited. *J. Phys. Chem. B* **2006**, *110*, 15700–15707.

(9) Scarabelli, L.; Coronado-Puchau, M.; Giner-Casares, J. J.; Langer, J.; Liz-Marzán, L. M. Monodisperse gold nanotriangles: Size control, large-scale self-assembly, and performance in surface-enhanced Raman scattering. *ACS Nano* **2014**, *8*, 5833–5842.

(10) Zhou, J.; An, J.; Tang, B.; Xu, S.; Cao, Y.; Zhao, B.; Xu, W.; Chang, J.; Lombardi, J. R. Growth of tetrahedral silver nanocrystals in aqueous solution and their SERS enhancement. *Langmuir* **2008**, *24*, 10407–10413.

(11) Schmidt, M. S.; Hübner, J.; Boisen, A. Large area fabrication of leaning silicon nanopillars for surface enhanced Raman spectroscopy. *Adv. Mater.* **2012**, *24*, OP11–OP18.

(12) Daglar, B.; Khudiyev, T.; Demirel, G. B.; Buyukserin, F.; Bayindir, M. Soft biomimetic tapered nanostructures for large-area antireflective surfaces and SERS sensing. *J. Mater. Chem. C* **2013**, *1*, 7842–7848.

(13) Zhang, C.-L.; Lv, K.-P.; Cong, H.-P.; Yu, S.-H. Controlled assemblies of gold nanorods in PVA nanofiber matrix as flexible free-standing SERS substrates by electrospinning. *Small* **2012**, *8*, 648–653.

(14) Green, M.; Liu, F. M. SERS substrates fabricated by island lithography: the silver/pyridine system. *J. Phys. Chem. B* **2003**, *107*, 13015–13021.

(15) Zheng, G.; Polavarapu, L.; Liz-Marzán, L. M.; Pastoriza-Santos, I.; Pérez-Juste, J. Gold nanoparticle-loaded filter paper: A recyclable dip-catalyst for real-time reaction monitoring by surface enhanced Raman scattering. *Chem. Commun.* **2015**, *51*, 4572–4575.

(16) Focsan, M.; Carciun, A. M.; Potara, M.; Leordean, C.; Vulpoi, A.; Maniu, D.; Astilean, S. Flexible and tunable 3D gold nanocups platform as plasmonic biosensor for specific dual LSPR-SERS immuno-detection. *Sci. Rep.* **2017**, *7*, 14240.

(17) Park, M.; Jung, H.; Jeong, Y.; Jeong, K.-H. Plasmonic schirmer strip for human tear-based gouty arthritis diagnosis using surface-enhanced Raman scattering. *ACS Nano* **2017**, *11*, 438–443.

(18) Alvarez-Puebla, R. A.; Agarwal, A.; Manna, P.; Khanal, B. P.; Aldeanueva-Potel, P.; Carbó-Argibay, E.; Pazos-Pérez, N.; Vigderman, L.; Zubarev, E. R.; Kotov, N. A.; Liz-Marzán, L. M. Gold nanorods 3D-supercrystals as surface enhanced Raman scattering spectroscopy substrates for the rapid detection of scrambled prions. *Proc. Natl. Acad. Sci.* **2011**, *108*, 8157–8161.

(19) Bontempi, N.; Carletti, L.; De Angelis, C.; Alessandri, I. Plasmon-free SERS detection of environmental CO_2 on TiO_2 surfaces. *Nanoscale* **2016**, *8*, 3226–3231.

(20) Qi, D.; Lu, L.; Wang, L.; Zhang, J. Improved SERS sensitivity on plasmon-free TiO_2 photonic microarray by enhancing light-matter coupling. *J. Am. Chem. Soc.* **2014**, *136*, 9886–9889.

(21) Ling, X.; Wu, J.; Xie, L.; Zhang, J. Graphene-thickness-dependent graphene-enhanced Raman scattering. *J. Phys. Chem. C* **2013**, *117*, 2369–2376.

(22) Alessandri, I. Enhancing Raman scattering without plasmons: Unprecedented sensitivity achieved by TiO_2 shell-based resonators. *J. Am. Chem. Soc.* **2013**, *135*, 5541–5544.

(23) Xie, L.; Ling, X.; Fang, Y.; Zhang, J.; Liu, Z. Graphene as a substrate to suppress fluorescence in resonance Raman spectroscopy. *J. Am. Chem. Soc.* **2009**, *131*, 9890–9891.

(24) Ling, X.; Zhang, J. First-layer effect in graphene-enhanced Raman scattering. *Small* **2010**, *6*, 2020–2025.

(25) Liu, D. et al. Raman enhancement on ultra-clean graphene quantum dots produced by quasi-equilibrium plasma-enhanced chemical vapor deposition. *Nat. Commun.* **2018**, *9*, 193.

(26) Novoselov, K. S.; Fal'ko, V. I.; Colombo, L.; Gellert, P. R.; Schwab, M. G.; Kim, K. A roadmap for graphene. *Nature* **2012**, *490*, 192–200.

(27) Golberg, D.; Bando, Y.; Huang, Y.; Terao, T.; Mitome, M.; Tang, C.; Zhi, C. Boron nitride nanotubes and nanosheets. *ACS Nano* **2010**, *4*, 2979–2993.

(28) Zhang, K.; Feng, Y.; Wang, F.; Yang, Z.; Wang, J. Two dimensional hexagonal boron nitride (2D-HBN): Synthesis, properties and applications. *J. Mater. Chem. C* **2017**, *5*, 11992–12022.

(29) Gravagnuolo, A. M.; Morales-Narváez, E.; Longobardi, S.; da Silva, E. T.; Giardina, P.; Merkoçi, A. In situ production of biofunctionalized few-layer defect-free microsheets of graphene. *Adv. Funct. Mater.* **2015**, *25*, 2771–2779.

(30) Kaur, J.; Vergara, A.; Rossi, M.; Gravagnuolo, A. M.; Valadan, M.; Corrado, F.; Conte, M.; Gesuele, F.; Giardina, P.; Altucci, C. Electrostatically driven scalable synthesis of MoS_2-graphene hybrid films assisted by hydrophobins. *RSC Adv.* **2017**, *7*, 50166–50175.

(31) Li, L. H.; Chen, Y. Atomically thin boron nitride: Unique properties and applications. *Adv. Funct. Mater.* **2016**, *26*, 2594–2608.

(32) Mirbagheri, M.; Hwang, D. K. The coffee-ring effect on 3D patterns: A simple approach to creating complex hierarchical materials. *Adv. Mater. Interfaces* **2019**, 1900003.

(33) Kim, P.; Abkarian, M.; Stone, H. A. Hierarchical folding of elastic membranes under biaxial compressive stress. *Nat. Mater.* **2011**, *10*, 952–957.

(34) Hughes, B. R.; Mirbagheri, M.; Waldman, S. D.; Hwang, D. K. Direct cell-cell communication with three-dimensional cell morphology on wrinkled microposts. *Acta Biomater.* **2018**, *78*, 89–97.

(35) Rofouie, P.; Pasini, D.; Rey, A. D. Multiple-wavelength surface patterns in models of biological chiral liquid crystal membranes. *Soft Matter* **2017**, *13*, 541–545.

(36) Fetters, L. J.; Lohse, D. J.; Richter, D.; Witten, T. A.; Zirkel, A. Connection between polymer molecular weight, density, chain dimensions, and melt viscoelastic properties. *Macromolecules* **1994**, *27*, 4639–4647.

(37) Li, M.; Joung, D.; Hughes, B.; Waldman, S. D.; Kozinski, J. A.; Hwang, D. K. Wrinkling non-spherical particles and its application in cell attachment promotion. *Sci. Rep.* **2016**, *6*, 30463.

(38) Blake, P.; Hill, E. W. Making graphene visible. *Appl. Phys. Lett.* **2007**, *91*, 063124.

(39) Metten, D.; Froehlicher, G.; Berciaud, S. Doping- and interference-free measurement of I_{2D} / I_G in suspended monolayer graphene blisters. *phys status solidi (b)* **2015**, *252*, 2390–2394.

(40) Wu, J.-B.; Lin, M.-L.; Cong, X.; Liu, H.-N.; Tan, P.-H. Raman spectroscopy of graphene-based materials and its applications in related devices. *Chem. Soc. Rev.* **2018**, *47*, 1822–1873.

(41) Griffin, A.; Harvey, A.; Cunningham, B.; Scullion, D.; Tian, T.; Shih, C.-J.; Gruening, M.; Donegan, J. F.; Santos, E. J. G.; Backes, C.; Coleman, J. N. Spectroscopic size and thickness metrics for liquid-exfoliated h-BN. *Chem. Mater.* **2018**, *30*, 1998–2005.

(42) Abdelkarim, O.; Kaur, J.; Liu, J.; Navarro-Pardo, F.; Zarrin, H.; Yurtsever, A.; Bassioni, G.; Wang, Z. M.; Selopal, G. S.; Rosei, F. Two-dimensional functionalized hexagonal boron nitride for quantum dot photoelectrochemical hydrogen generation. *J. Mater. Chem. A* **2020**, DOI: 10.1039/D0TA05260D.

(43) Ferrari, A. C.; Meyer, J. C.; Scardaci, V.; Casiraghi, C.; Lazzeri, M.; Mauri, F.; Piscanec, S.; Jiang, D.; Novoselov, K. S.; Roth, S.; Geim, A. K. Raman spectrum of graphene and graphene layers. *Phys. Rev. Lett.* **2006**, *97*, 187401.

(44) Stenberg, H.; Matikainen, A.; Daniel, S.; Nuutinen, T.; Stenberg, P.; Honkanen, S.; Pakkanen, T.; Vahimaa, P.; Suvanto, M. Self-organized polymer wrinkles: A lithography-free pathway for surface-enhanced Raman scattering (SERS) substrates. *Macromol. Mater. Eng.* **2015**, *300*, 386–390.

(45) Valeš, V.; Drogowska-Hornà, K.; Guerra, V. L. P.; Kalbàč, M. Graphene-enhanced Raman scattering on single layer and bilayers of pristine and hydrogenated graphene. *Sci. Rep.* **2020**, *10*, 4516.

(46) Lee, J.; S., N. K.; Shin, H. S. Interaction between metal and graphene: dependence on the layer number of graphene. *ACS Nano* **2010**, *5*, 608–612.

(47) Li, M.; Hakimi, N.; Perez, R.; Waldman, S.; Kozinski, J. A.; Hwang, D. K. Microarchitecture for a three-dimensional wrinkled surface platform. *Adv. Mater.* **2015**, *27*, 1880–1886.

TOC

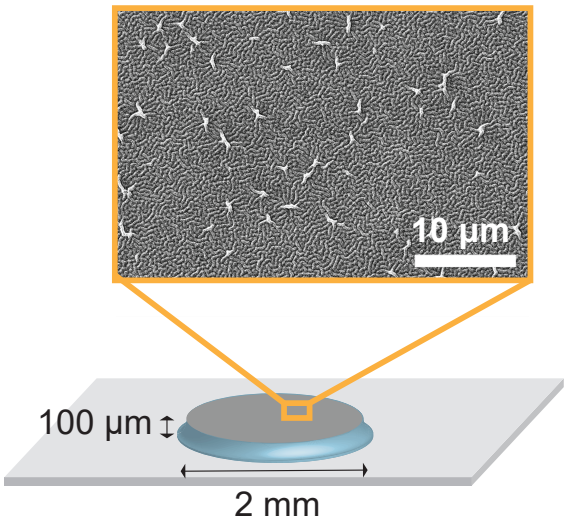

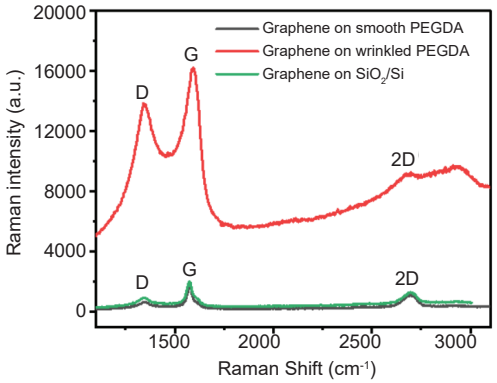

SERS of graphene on smooth and wrinkled PEGDA250 5 v% substrates as well as on a SiO_2/Si surface.

A facile approach is introduced for creating plasmon-free polymeric nanowrinkled substrates. The wrinkling wavelength can be reduced down to $\sim$ 375 nm by decreasing the polymer molecular weight and concentration. The significant improvement of SERS signals on the wrinkled patterns in comparison to those on the smooth PEGDA and Si/SiO_2 surfaces is demonstrated.